JOURNAL OF VIROLOGY, Dec. 1990, p. 5716–5729
0022-538X/90/125716-14$02.00/0

Vol. 64, No. 12

Herpes Simplex Virus Particles Are Unable To Traverse the Secretory Pathway in the Mouse L-Cell Mutant gro29

BRUCE W. BANFIELD AND FRANK TUFARO*

Department of Microbiology, University of British Columbia, 300-6174 University Boulevard, Vancouver, British Columbia, Canada V6T 1W5

Received 4 May 1990/Accepted 3 September 1990

The mouse L-cell mutant gro29 was selected for its ability to survive infection by herpes simplex virus type 1 (HSV-1) and is defective in the propagation of HSV-1 and vesicular stomatitis virus (F. Tufaro, M. D. Snider, and S. L. McKnight, J. Cell Biol. 105:647–657, 1987). In this report, we show that gro29 cells harbor a lesion that inhibits the egress of HSV-1 virions during infection. We also found that HSV-1 glycoprotein D was slow to traverse the secretory pathway en route to the plasma membrane of infected gro29 cells. The movement of glycoproteins was not blocked entirely, however, and immunofluorescence experiments revealed that infected gro29 cells contained roughly 10% of the expected amount of glycoprotein D on their cell surface at 12 h postinfection. Furthermore, nucleocapsids and virions assembled inside the cells during infection, suggesting that the lesion in gro29 cells impinged on a late step in virion maturation. Electron micrographs of infected cells revealed that many of the intracellular virions were contained in irregular cytoplasmic vacuoles, similar to those that accumulate in HSV-1-infected cells treated with the ionophore monensin. We conclude from these results that gro29 harbors a defect that blocks the egress of HSV-1 virions from the infected cell without seriously impeding the flux of individual glycoproteins to the cell surface. We infer that HSV-1 maturation and egress require a host cell component that is either reduced or absent in gro29 cells and that this lesion, although not lethal to the host cell, cannot be tolerated by HSV-1 during its life cycle.

Enveloped viruses that infect mammalian cells require the host cell secretory pathway for the transport and processing of membrane proteins that are utilized during the course of virus assembly. In addition, there is evidence to suggest that several animal viruses, including herpes simplex virus (21), mouse hepatitis virus (47, 48), Uukuniemi virus (28–30), and Berne virus (52) interact directly with secretory organelles such as the Golgi complex during their life cycle. While significant progress has been made in understanding the mechanisms that regulate the synthesis, processing, and sorting of newly made secreted and membrane glycoproteins in the cell, less is known about how viruses interact with the components of the secretory apparatus.

One way to identify these interactions is to isolate mutant cell lines with defects in cellular components required for the synthesis and transport of integral membrane glycoproteins. This approach has been useful for studying the properties of viral and nonviral proteins and also for investigating the effects of these mutations on virus production (7, 10, 14–18, 24–26, 34, 49; for a review, see reference 46). In addition, several of these mutant cell lines have been essential to the development of in vitro assays designed to study transport between cellular compartments (2–5, 36).

In a previous study, a mouse L-cell mutant termed gro29 was isolated (50) and shown to be defective in the growth of two enveloped viruses, vesicular stomatitis virus (VSV), which buds from the plasma membrane, and herpes simplex virus type 1 (HSV-1), which buds from the inner lamellae of the nuclear membrane (13, 33, 35). Initial characterization of this cell line showed that VSV-infected gro29 cells were defective in the transport and processing of newly made G protein, the envelope glycoprotein of VSV. Despite this defect, the release of infectious VSV from gro29 cells was diminished only threefold when compared with the normal parental L cells, suggesting that the secretory defect in this cell line was not critical for the maturation and egress of VSV from the plasma membrane. The effect of this lesion on the release of infectious HSV-1 was very different, however. Although gro29 cells were infected efficiently and the replication cycle proceeded to the late stages of viral gene expression, the spread of HSV-1 from cell to cell did not occur and underprocessed glycoproteins accumulated inside the gro29 cells at late times of infection (50).

In contrast to VSV, which encodes a single glycoprotein, at least seven virally encoded membrane glycoproteins are synthesized during HSV-1 infection in culture: gB, gC, gD, gE, gG, gH, and gI (1, 6, 20, 31, 37, 45). It is now well established that pharmacologic agents or cellular mutations that affect glycoprotein processing or transport affect the formation, and to a lesser extent, the egress of infectious herpes simplex virus particles in infected cells (10, 21, 50). During the maturation of HSV-1 in culture, nucleocapsids bud at the nuclear membrane and acquire an envelope comprising predominantly immature forms of the virus-encoded glycoproteins (12). The virions that exit from the cell contain mature, highly processed forms of the same glycoproteins. These observations have led to a model for HSV-1 egress in which the envelope glycoproteins are processed while resident in the viral envelope and are exposed to the host cell processing machinery as the virus traverses the secretory apparatus en route out of the cell (21, 45). The rules governing the trafficking to the cell surface of individual HSV-1 glycoproteins versus newly assembled virions have not been elucidated.

To further our understanding of the virus-host interactions governing these processes, we investigated the nature of the block to virus production in the gro29 cell line. In this report, we demonstrate that the rate of transport and processing of HSV-1 glycoproteins from their site of synthesis in the

* Corresponding author.

endoplasmic reticulum (ER) to the cell surface was impeded in infected gro29 cells. This defect in protein transport reduced but did not eliminate the appearance of viral glycoproteins in the plasma membrane of the infected cells. In contrast, newly assembled virions failed to exit the host cell. In infected gro29 cells, the intracellular virions contained predominantly immature forms of the envelope glycoproteins and accumulated in cytoplasmic vacuoles resembling those that accumulate in cells treated with the carboxylic ionophore monensin, which also blocks HSV-1 egress (21). The phenotype of the gro29 mutant cell line is unique with regard to HSV-1 infection, and our experiments suggest that HSV-1 requires a host cell component for efficient virus maturation and egress that is distinct from those components which facilitate the trafficking of viral membrane glycoproteins.

MATERIALS AND METHODS

Abbreviations used. DMEM, Dulbecco modified Eagle medium; endo H, endoglycosidase H; FBS, fetal bovine serum; hpi, hours postinfection; MOI, multiplicity of infection; PFU, plaque-forming unit; TCA, trichloroacetic acid; SDS, sodium dodecyl sulfate; NP-40, Nonidet P-40; gD, glycoprotein D.

Cells and viruses. Parental cells were the clone 1D line of LMtk$^-$ mouse fibroblasts. The mutant gro29 cell line was obtained by mutagenesis of the L-cell line with ethylmethane sulfonate and selected for the ability to survive HSV-1 infection (50). Vero cells were a kind gift from S. McKnight. All cells were grown at 37°C in DMEM supplemented with 10% FBS in a 5% CO_2 atmosphere. The virus used was the HSV-1 KOS strain, a kind gift from D. Coen. Anti-HSV-1 antibodies were kind gifts from M. Zweig and R. Philpotts.

Harvesting of virus. Medium was removed from infected-cell monolayers and subjected to low-speed centrifugation to pellet cell debris. The supernatant was centrifuged for 2 h at 20,000 × *g* to pellet the virions, and the resulting pellet was suspended in 10 mM Tris (pH 7.8)–50 mM NaCl on ice. This material was sedimented through a 5 to 40% dextran T10 gradient formed in 50 mM NaCl–10 mM Tris (pH 7.8) for 1 h at 22,000 rpm in a Beckman SW41 rotor. Gradients were fractionated from the bottom of the tube into 0.5-ml fractions. For determination of radioactivity in insoluble material, 10% of each fraction to be analyzed was added to 50 μg of bovine serum albumin followed by 1 ml of 10% cold TCA. Insoluble material was collected onto filters after 1 h, and radioactivity was determined by scintillation counting. For determination of virus titers, fractions were diluted serially with medium and used to inoculate monolayers of Vero cells growing in 96-well dishes. Microtiter wells were scored, and titers were calculated when a generalized cytopathic effect was noticed in control infected samples. For electrophoretic analyses, samples of fractions to be analyzed were centrifuged at 436,000 × *g* for 20 min in a Beckman TLA 100.2 rotor. Pelleted material was solubilized in SDS sample buffer and subjected to SDS-polyacrylamide gel electrophoresis. Following electrophoresis, gels were fixed and dried and autoradiography was performed. In some cases, gels were transferred to nitrocellulose membranes for Western blot (immunoblot) analysis prior to autoradiography.

Determination of virus titer. Medium was removed completely from infected-cell monolayers at various sampling times and replaced with fresh medium. Each sample medium to be titered was centrifuged to remove cell debris. Serial 10-fold dilutions of each sample were made and used to inoculate confluent monolayers of Vero cells. After 1 h, the inoculum was removed and the monolayers were overlaid with fresh DMEM containing 4% FBS and 0.8% agar or Methocell. Duplicate wells for each sample were analyzed after 3 and 5 days.

Pulse-chase labeling experiments. Monolayers of L cells and gro29 cells were infected with HSV-1 (MOI = 10). After 1 h, the virus was removed and replaced with complete medium. At 5 hpi, cells were washed three times with methionine-free medium and labeled for 30 min with [^{35}S]methionine (Dupont) at 100 μCi/ml in methionine-free medium containing 5% dialyzed FBS. At the completion of labeling, cells were either harvested immediately or washed three times and incubated in DMEM containing excess methionine for various times. Cells were harvested by washing the monolayer with cold phosphate-buffered saline and incubated for 15 min with cold lysis buffer (10 mM Tris hydrochloride [pH 7.4], 150 mM NaCl, 1% NP-40, 1% sodium deoxycholate).

Immunoprecipitations. One-tenth the volume of 10% NP-40–10% sodium deoxycholate–1% SDS was added to samples of cell lysates to be precipitated. The appropriate volume of anti-HSV-1 gD monoclonal antibody was added to each aliquot and the sample was incubated overnight on ice. A 10% suspension of *Staphylococcus aureus* cells was then added to each sample equal to 20 volumes of primary antibody. This mixture was rocked at 4°C for 2 h before the cells were pelleted and washed three times successively with 0.5 ml of the following solutions: wash buffer 1 (20 mM Tris hydrochloride [pH 7.5], 150 mM NaCl, 1% NP-40), wash buffer 2 (20 mM Tris hydrochloride [pH 8.8], 150 mM NaCl, 1% NP-40, 0.2% SDS), and wash buffer 3 (20 mM Tris hydrochloride [pH 6.8], 150 mM NaCl, 1% NP-40, 0.2% SDS). The final pellet was suspended in SDS sample buffer, heated at 100°C for 5 min, and subjected to electrophoresis in a 10% SDS–polyacrylamide gel. Gels were fixed, dried, and exposed to Kodak XAR-5 film for autoradiography.

Endo H digestions. The *S. aureus* pellets were suspended in 40 μl of 2× endo H buffer (1% SDS, 5% β-mercaptoethanol, 2 mM NaN_3, 100 mM sodium citrate [pH 5.5]), heated at 100°C for 5 min and centrifuged to pellet the cells, and the supernatants were transferred to a fresh tube. Each supernatant was divided into two tubes containing 20 μl of distilled H_2O. The material was then digested or mock digested for 18 h at 37°C by the addition of 1 mU of endo H or 1 μl of distilled H_2O. Samples were subjected to polyacrylamide gel electrophoresis, and autoradiography was performed as described above.

Western blots. Cellular extracts were subjected to SDS-polyacrylamide gel electrophoresis and electroblotted to nitrocellulose membranes. Proteins were visualized using monoclonal antibodies and an alkaline phosphatase-based detection kit from GIBCO/BRL, Ontario, Canada.

Fractionation of microsomes. This procedure was adapted from Saraste et al. (40). Briefly, monolayers of infected or uninfected cells were harvested by trypsinization, and the trypsin was quenched by the addition of cold DMEM containing 10% FBS. All further steps were carried out in the cold. Cells were pelleted by centrifugation for 10 min, washed with DMEM containing 10% FBS, followed by a wash with homogenization buffer (0.25 M sucrose, 10 mM Tris [pH 7.4], 10 mM KCl, 1.5 mM $MgCl_2$). Cells were then pelleted, resuspended in 4 volumes of homogenization buffer, and homogenized in a Dounce homogenizer. Nuclei and cell debris were removed from the homogenate by centrifugation. The pellet was then washed with homogeni-

zation buffer, and the supernatants were combined. This was centrifuged at 10,000 × *g* for 20 min to remove mitochondria. The postmitochondrial supernatant was then decanted and layered on top of 5 ml of 0.33 M sucrose, which in turn was layered over 1 ml of 2 M sucrose. This was centrifuged at 25,000 rpm in a SW41 rotor for 1 h. Approximately 600 μl of the turbid band at the 2 M-0.33 M interface was removed with a syringe. This material was suitable for further purification of Golgi membranes. This total microsome sample was made 50% in sucrose with the addition of 2.4 ml of 2 M sucrose and was added to an SW41 tube. The following sucrose solutions (wt/wt) were layered on top: 1 ml of 45%; 1.5 ml each of 40, 35, 30, and 25%; and 2 ml of 20%. The step gradients were then centrifuged at 170,000 × *g* for 19 h. Following centrifugation, 0.5-ml fractions were collected from the bottom of the tube. About 0.15 ml of each fraction was diluted with 0.5 ml of distilled H_2O and centrifuged at 436,000 × *g* for 10 min. The supernatants were discarded, and the pellets were suspended in 30 μl of SDS sample buffer, boiled for 5 min, and subjected to polyacrylamide gel electrophoresis. Polypeptides were transferred to nitrocellulose by Western blotting, and specific polypeptides were detected by using monoclonal antibodies as described above. The density of the fractions ranged from 1.08 to 1.24. The location of the intermediate compartment between the ER and the Golgi was determined by Western blotting, using an anti-p58 monoclonal antibody. This served as a useful marker for the location of this compartment. In our hands, this fractionation procedure yields a protein peak in fraction 5 and a peak of the ER marker NADPH cytochrome *c* reductase in fraction 4.

Flow cytometry. Monolayers of L and gro29 cells were grown on 10-cm-diameter dishes for 24 h. Cells were infected with HSV-1 (MOI = 10) or mock infected and incubated for 12 h. Monolayers were then washed to remove free virus in the medium and removed from the dish by incubating with DMEM containing 5 mM EDTA. Cells were washed two times in FACS buffer (0.5% BSA, 20 mM *N*-2-hydroxyethylpiperazine-*N'*-2-ethanesulfonic acid [HEPES] [pH 7.2], 20 mM NaN_3, in DMEM) and suspended in FACS buffer containing anti-gD monoclonal antibody. After 45 min at 18°C, cells were washed two times in FACS buffer and suspended in FACS buffer containing fluorescein isothiocyanate-conjugated goat anti-mouse antibody. After 45 min at 18°C, cells were washed extensively in FACS buffer, fixed in 1.5% paraformaldehyde, and analyzed by using a Becton-Dickinson FACScan. Data from 10^4 cells were plotted in linear and log scale using the FACScan software and used to calculate the average fluorescence intensity of infected and uninfected cells.

Indirect immunofluorescence. Cells were grown on glass cover slips for 3 days and infected with HSV-1 (MOI = 5). At 13 hpi, cells were rinsed, fixed with 3% formaldehyde in phosphate-buffered saline, and incubated with a 1/100 dilution of anti-gD monoclonal antibody. Monolayers were washed extensively and incubated with 1/100 dilution of rhodamine-conjugated goat anti-mouse immunoglobulin G for 30 min. Cover slips were then washed and mounted in 50% glycerol–100 mM Tris (pH 7.8). Images were photographed using a Zeiss microscope with epifluorescence optics. Confocal images were captured using a Bio-Rad MRC-500 confocal fluorescence microscope.

Electron microscopy. Cells were grown on Millicell HA inserts (Millipore Corporation) for 24 h prior to infection with HSV-1 (MOI = 5). At 18 hpi, cells were rinsed with phosphate-buffered saline and monolayers were fixed in 2.5% glutaraldehyde in 0.1 M sodium cacodylate (pH 7.3) for 1 h on ice. Cells were then rinsed and postfixed in 1% OsO_4 for 1 h. These samples were rinsed, dehydrated, and embedded in plastic. Specimens were sectioned, stained, and photographed by using a Zeiss EM10C transmission electron microscope.

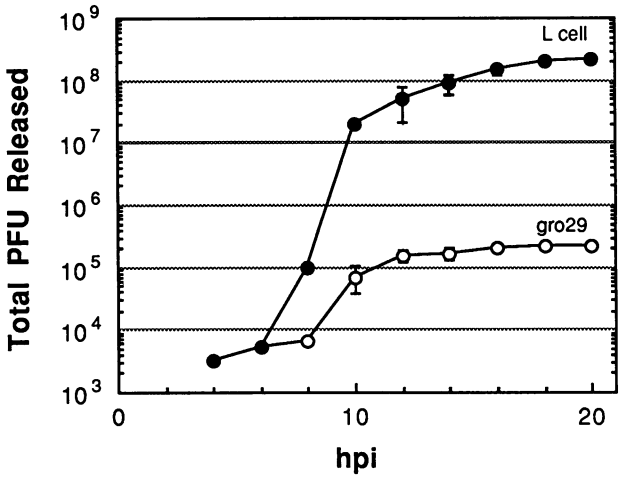

FIG. 1. Titer of virus released from HSV-1-infected L and gro29 cells. Monolayers of L and gro29 cells were infected with HSV-1 (MOI = 10). At the indicated times postinfection, the medium was removed and the numbers of infectious particles were determined by plaque assay on Vero cells as described in Materials and Methods.

RESULTS

Production of infectious virus by gro29 cells. It has been shown previously by indirect immunofluorescence that plaques do not form on monolayers of gro29 cells infected with HSV-1, despite the fact that infection occurs normally and progresses to the late stages of viral gene expression (50). To quantify the block to viral propagation in gro29 cells, the titers of the extracellular virus produced by infected parental L cells and gro29 cells were determined. The medium on each monolayer was replaced every 2 hpi to minimize the superinfection of cells during the experiment. The titers were determined for each time point and then added together to reflect the total number of PFU released from the cells during the 20 h of sampling (Fig. 1). These analyses revealed that the parental L cells released 200 PFU per cell, while gro29 cells released 0.1 PFU per cell. There are several possibilities that could account for this deficiency. If viral assembly or egress were defective, the release of virions from gro29 cells would be impaired. If the assembly and egress of the virions were normal, it may be that the specific infectivity of the virus was diminished due to a structural defect caused by a lesion in the gro29 cells.

It has already been established that gro29 cells have suffered a defect in glycoprotein transport and processing that leads to the accumulation of immature forms of HSV-1 glycoproteins in HSV-1-infected cells (50). Because of the importance of the viral glycoproteins to the propagation of HSV-1 (for a review, see reference 45), experiments were carried out to identify the defects in glycoprotein processing and to characterize the phenomena that contribute to the low yield of infectious virus from the gro29 cell line.

Pulse-chase analysis of HSV-1 glycoprotein processing. HSV-1 specifies at least seven membrane glycoproteins: gB,

gC, gD, gE, gG, gH, and gI (1, 6, 20, 31, 37, 45). We chose to investigate gD and gB in these experiments. gD contains three sites for N-linked oligosaccharides (11) and two O-linked chains (43), whereas gB has nine potential N-linked sites (8) and an uncharacterized number of O-linked chains. The precursor forms of these proteins (pgB and pgD) contain high-mannose oligosaccharides sensitive to endo H which become resistant to endo H as the oligosaccharide moieties are processed to more-complex forms (9, 11, 22, 32, 42, 53).

To investigate the synthesis and processing of these proteins, pulse-chase analyses of the two glycoproteins in HSV-1-infected cells were performed at 5 hpi (Fig. 2A). When HSV-1-infected parental L cells and gro29 mutant cells were labeled with [^{35}S]methionine for 10 min, the rates of synthesis of gB and gD were similar for both cell lines.

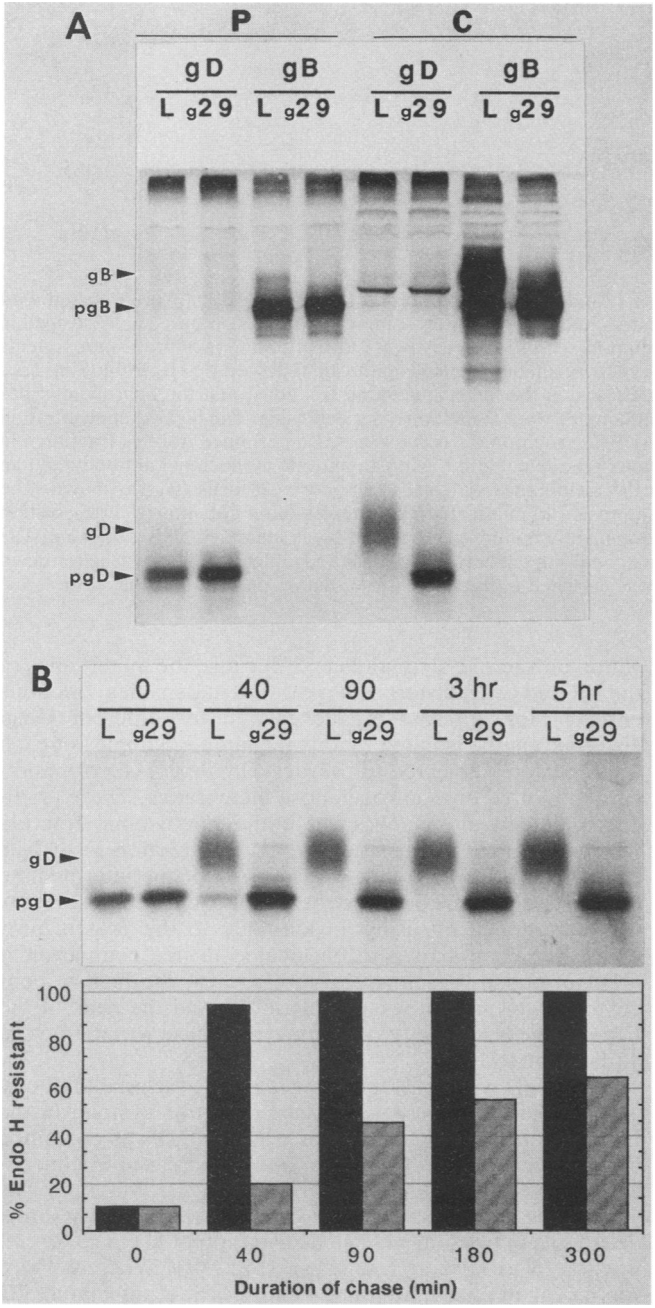

The major bands representing the newly synthesized gD in L and gro29 cells had the same relative mobilities in the gel, indicating that the co- and posttranslational modifications, such as the addition of N-linked oligosaccharides, occurred normally in both cell lines. Similarly, the synthesis and processing of gB in the two cell lines were indistinguishable at the end of the labeling period. After a 90-min chase in the parental L cells (Fig. 2A), both gB and gD migrated more slowly in the gels, suggesting that processing of the high-mannose oligosaccharides to complex forms as well as modification by O-linked glycosylation had occurred. By contrast, most of the gB and gD polypeptides synthesized in gro29 cells did not increase in size during the chase. There was no reduction in the amount of labeled polypeptides in the cells during the chase period, indicating that the bulk of newly made material persisted in forms that were incompletely or aberrantly processed. The increase in radioactivity observed in several chase samples (L-cell chase, gB for example) may be due to more efficient immunoprecipitation of those species.

Several explanations could account for the failure to modify newly made glycoproteins in this cell line. The underprocessed species in the mutant gro29 cells may represent glycoproteins that were retained in the ER or Golgi. Alternatively, the newly synthesized polypeptides may have traversed the Golgi without being processed. This could arise if a component of the ER- or Golgi-resident processing machinery were defective in these cells. The following experiments were done to characterize further the glycoprotein flux through the Golgi complex. Pulse-chase analyses of gD were repeated using a longer chase, and the rates at which newly made glycoproteins became endo H resistant were determined (Fig. 2B). Because endo H cleaves high-mannose chains but not complex oligosaccharides, it serves as a useful probe for the processing of N-linked glycoproteins (27). gD was chosen for further analysis because all mature forms of this protein are endo H resistant, whereas at least some of the high-mannose N-linked oligosaccharides attached to gB remain in a sensitive form (22, 53). Newly made gD was processed rapidly in L cells; by 40 min postlabeling, greater than 95% of the polypeptides were modified to a higher apparent molecular weight, and by 90 min, processing was complete (Fig. 2B). By contrast, gD synthesized in gro29 cells failed to become fully processed even after a 5-h chase. By 40 min, two or three discrete bands were detected that were larger than pgD, indicating that some modifications had occurred, although a compari-

FIG. 2. Processing of HSV-1 gD and gB in L and gro29 cells. Monolayers of L and gro29 cells were infected with HSV-1 (MOI = 10). At 5 hpi, cells were incubated with [^{35}S]methionine for 10 min, rinsed, and chased with unlabeled methionine for 90 min. HSV-1 gD and gB were immunoprecipitated from total cell extracts using appropriate monoclonal antibodies and subjected to SDS-polyacrylamide gel electrophoresis. (A) Autoradiogram showing HSV-1 gD and gB at the end of the labeling period (P) or after a 90-min chase (C) in L cells (L) and gro29 cells (g29) as indicated. The positions of immature forms of gB and gD (pgB and pgD) and mature forms (gB and gD) are indicated to the left of the gel. (B) (top) Autoradiogram showing pulse-chase analysis of HSV-1 gD. The positions of pgD and gD and the duration of chase (in minutes or hours) are indicated. (bottom) Histogram showing the percent of HSV-1 gD (top panel) that was resistant to digestion by endo H. Samples from pulse-chase experiments were digested with endo H and subjected to SDS-polyacrylamide gel electrophoresis. The relative amounts of endo H-resistant gD was determined by densitometric scanning of autoradiograms. Symbols: ■, L cells; ▨, gro29 cells.

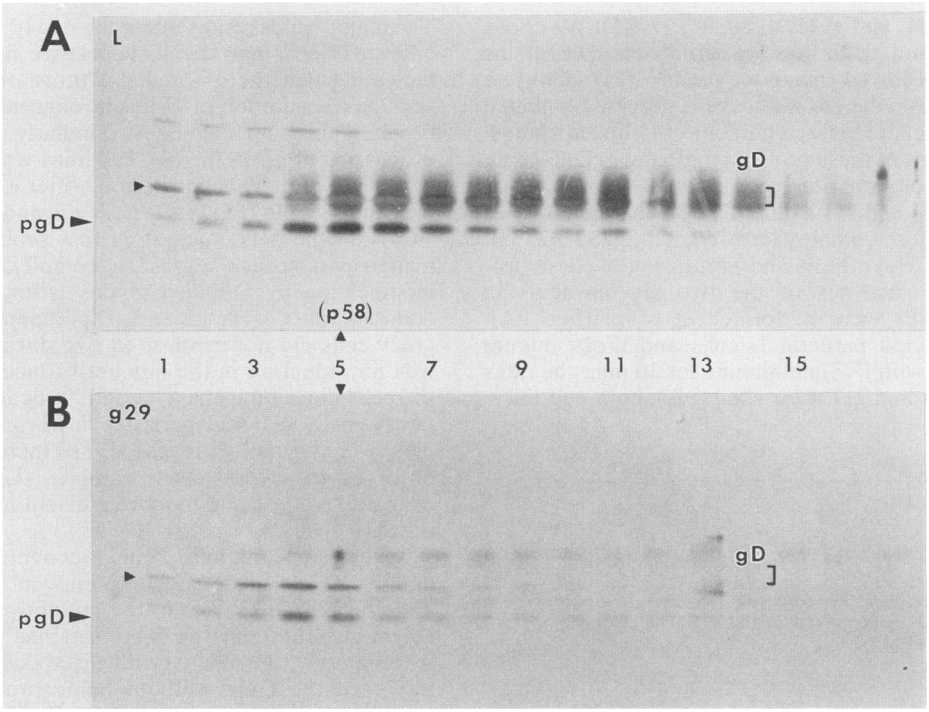

FIG. 3. Western blot analysis of HSV-1 gD in membrane fractions of L and gro29 cells. Parental L and gro29 cells were infected with HSV-1 (MOI = 10) and incubated for 13 h. Cell monolayers were harvested, and the total microsome fraction was prepared as described in Materials and Methods. Total microsomes were subjected to centrifugation in sucrose step gradients to fractionate membrane components of different densities. Fractions were solubilized and subjected to SDS-polyacrylamide gel electrophoresis followed by electroblotting onto a nitrocellulose membrane. The dense membranes characteristic of the ER are in the lower numbered fractions, and the light membranes characteristic of the Golgi complex are in the higher numbered fractions. Samples were loaded on a per cell basis. The highest concentration of protein was in fraction 4, and the peak activity of the ER enzyme NADPH cytochrome *c* reductase was determined to be in fraction 4 in gradients similar to those shown. The HSV-1 gD present in these fractions was detected by using an anti-gD monoclonal antibody and an alkaline phosphatase staining procedure. Western blots showing gD in the membranes of L cells (A) and gro29 cells (B) are shown. The arrowhead in the leftmost lane denotes a background band that was also present in uninfected-cell samples (data not shown). The position of pgD is indicated to the left of the gel, and the sample containing predominantly mature gD (fraction 14) is identified above the lane. The location of p58, a protein that has been shown to reside in the intermediate compartment between the ER and Golgi complex, was determined on separate blots by using an anti-p58 antibody (data not shown). p58 was enriched in fractions 4 to 6, with a peak in fraction 5.

son of relative mobilities suggests that these were not the forms that accumulated in the parental L cells.

As the chase proceeded (Fig. 2B, bottom), there was a rapid and complete disappearance of endo H-sensitive forms in the L-cell samples, indicating that most of the mass of the newly made protein was modified by the host cell processing machinery. In contrast, the gD synthesized in gro29 cells persisted as endo H-sensitive forms. Oligosaccharide processing was not blocked entirely, however, and 60% of the newly synthesized gD acquired endo H resistance during the 5-h chase (Fig. 2B). These results indicate that the intracellular transport of HSV-1 glycoproteins was slowed but not abolished in infected gro29 cells. The large shift in molecular weight that accompanies the maturation of gD in L cells was not observed in the gro29 cell samples. This is consistent with the notion that these modifications occur relatively late in the secretory pathway, after the acquisition of endo H resistance.

Analysis of gD transport in HSV-1-infected cells. The data obtained from the pulse-chase analysis suggested that the transport of glycoproteins through the secretory pathway of gro29 cells was abnormal. To investigate the accumulation of glycoproteins in the organelles of the secretory pathway during HSV-1 infection, total microsomes were prepared from infected cells at 13 hpi and were subjected to centrifugation on sucrose step gradients. Because the membranes of the ER and Golgi cisternae have different densities, fractions enriched for different organelles and for different Golgi cisternae can be isolated by this technique. Samples of each fraction were subjected to polyacrylamide gel electrophoresis and blotted onto nitrocellulose membranes. These gradients included all membranes in the microsomal fraction which separated at densities from 1.24 (fraction 1) to 1.08 (fraction 15). Furthermore, the location of the intermediate compartment that exists between the ER and Golgi complex was determined by using an antibody to the protein p58, which has been shown to be located in this compartment (41). In gradients similar to those shown, the highest concentration of protein was in fraction 5, and the peak of the ER enzyme NADPH cytochrome *c* reductase was in fraction 4 (data not shown).

HSV-1 gD was analyzed by using a monoclonal antibody and an alkaline phosphatase-based detection system. In the L-cell samples (Fig. 3A), the majority of pgD was contained in four fractions (fractions 4 to 7) and decreased in concentration towards the top of the gradient (right). Mature forms of gD were detectable by fraction 4 and were the only forms detectable in fraction 14. The distribution of gD in gro29 cell fractions was strikingly different (Fig. 3B). Whereas there was a peak of pgD in fractions 4 and 5, little if any mature gD

fractionated in the gro29 cell gradient. It was evident that gro29 fractions contained less gD overall than did L-cell fractions, although the differences were not quantified in these experiments. When these same blots were probed for the presence of the Golgi marker p58, a protein that is enriched in the intermediate compartment between the ER and Golgi complex (41), p58 was equally abundant in the gro29 cell and L-cell fractions, suggesting that the underrepresentation of gD in the gro29 cell fractions was not an artifact of the isolation procedure. This suggests that gD was underrepresented in the cellular organelles contained in these gradients. Because we have shown that the rate of synthesis of gD was normal in these cells (Fig. 2), it may be that the defect in gro29 cells caused gD to localize into abnormal cellular structures that were lost during this isolation procedure.

Analysis of virus egress. On the basis of the results demonstrating an inhibition of the transport and processing of HSV-1 glycoproteins and the underrepresentation of gD in the secretory organelles, we reasoned that the ability of HSV-1 particles to be transported out of the cell might also be impeded. This follows from the current model of HSV-1 egress in which newly formed virions are thought to traverse the Golgi complex en route out of the cell. To investigate this, parental L cells and gro29 cells were infected with HSV-1 and labeled with [^{35}S]methionine for 18 h. Extracellular virions were harvested from the medium by centrifugation and subjected to fractionation on dextran T10 gradients. The TCA-insoluble radioactivity was measured (Fig. 4A), and the titer of infectious particles was determined for each fraction (Fig. 4B). L cells released a large amount of virus which peaked in fraction 17 (Fig. 4A). In contrast, there was only a small peak of material detected in the gro29 cell medium (0.2% of L cell), indicating that virus release was impeded. An analysis of the PFU present in each fraction revealed that the peak of radioactivity (Fig. 4A, fractions 15, 16, and 17) corresponded to the peak of infectious virus (Fig. 4B). Fractions 15 to 17, comprising the peak in each gradient, were pooled and subjected to SDS-polyacrylamide gel electrophoresis (Fig. 4C). A limited number of radioactive bands were detected, consistent with these samples being highly enriched for virions. No radioactive polypeptides were detected in the gro29 samples during the exposure times used. We conclude from these data that gro29 cells are unable to release virions after infection.

To determine whether the secretion of all macromolecules from the mutant cells was impaired or whether there was a block specific for virion egress, the amount of TCA-insoluble radioactivity in the medium at the end of the 18-h labeling period was determined. During the course of the steady-state labeling, L cells secreted 2.1×10^7 cpm, while gro29 cells secreted 1.4×10^7 cpm in TCA-insoluble material, indicating that infected gro29 cells were able to secrete newly synthesized proteins efficiently. To test whether gro29 cells were able to secrete proteins late in infection, L and gro29 cells were infected with HSV-1 and incubated for 15 h in medium. Cells were then pulse-labeled for 30 min with [^{35}S]methionine, and the amounts of TCA-precipitable material secreted into the medium were determined. The medium was centri-

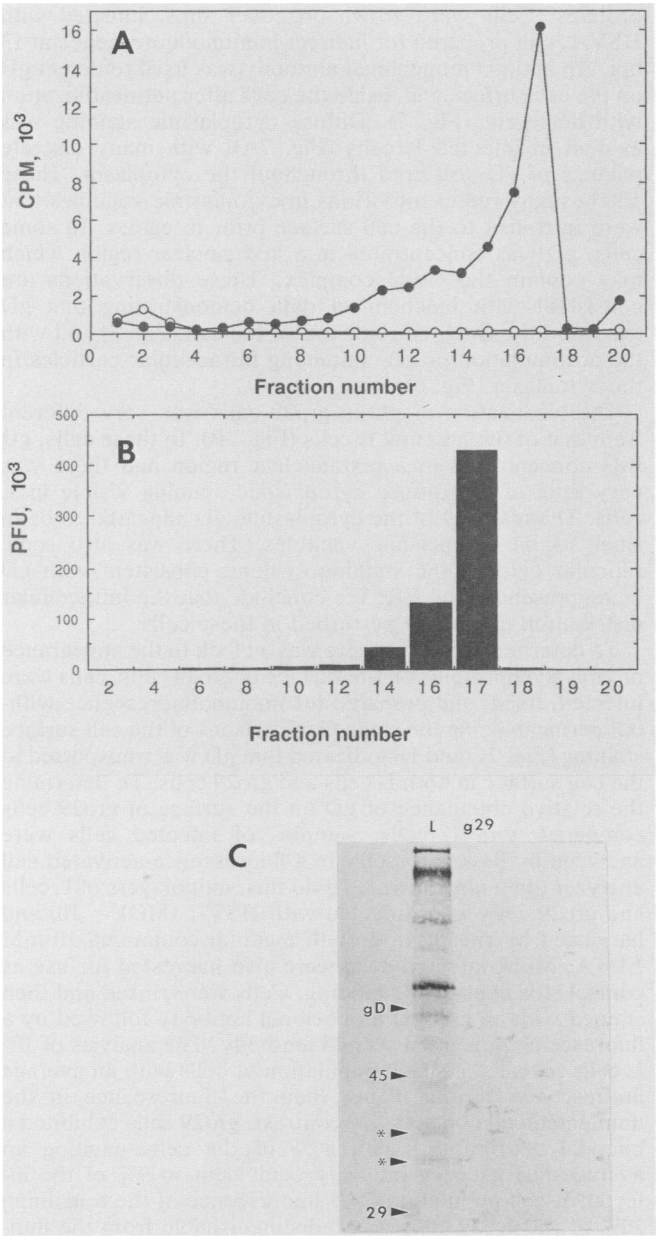

FIG. 4. Comparison of HSV-1 particles released from L and gro29 cells. Parental L cells and gro29 cells were infected with HSV-1 (MOI = 10). At 2 hpi, the medium was removed and replaced with labeling medium containing [^{35}S]methionine. At 18 hpi, virions released into the medium were harvested by centrifugation, suspended in buffer, and centrifuged through a 5 to 40% dextran T 10 gradient as described in Materials and Methods. The gradients were fractionated, and samples were retained for further analysis. Samples from the top of the gradient are shown to the left. (A) Total TCA-insoluble radioactivity in each sample. (B) Number of PFU in the fractions indicated. (C) Autoradiogram showing radioactive polypeptides present in the three peak fractions (fractions 15, 16, and 17) from each gradient. To prepare the samples, the fractions were pooled, pelleted by centrifugation, solubilized, and subjected to SDS-polyacrylamide gel electrophoresis. The polypeptides in the gel were electroblotted to nitrocellulose membranes, and viral proteins were identified using an anti-gD monoclonal antibody and an alkaline phosphatase detection system (data not shown). The blot was then exposed to film for 3 days to detect radioactive polypeptides in the pellets (shown in panel C). No signal was detectable for the gro29 sample. The positions of gD, nucleocapsid proteins (asterisks), and ovalbumin (45 kDa) and carbonic anhydrase (29 kDa) markers are shown.

fuged at 436,000 × g for 20 min to remove extracellular virions prior to TCA precipitation. In this assay, gro29 cells secreted 69% of the amount of TCA-insoluble radioactivity as did L cells. Taken together, these results indicate that virion egress and not secretion was blocked in gro29 cells. The specificity of this block likely accounts for the ability of gro29 cells to grow normally in culture.

Analysis of cell-associated virus. One explanation for the paucity of extracellular virions is if HSV-1 particles were unable to assemble in the mutant gro29 host cells. To investigate this, nucleocapsids were isolated from total cells and fractionated on sucrose gradients. Fractions were analyzed for TCA-insoluble radioactivity to detect the peak of nucleocapsids (Fig. 5A) and were subjected to polyacrylamide gel electrophoresis to detect nucleocapsid proteins (Fig. 5B and C). In Fig. 5A, a small peak of nucleocapsids was evident in fractions 22 to 29 for both L and gro29 cells. There were fewer nucleocapsids isolated from gro29 cells, although the reduction was minor when compared with the reduction in virion release. Polyacrylamide gel analysis of the gradient fractions (Fig. 5B and C) revealed that the patterns of newly made polypeptides in the nucleocapsid fractions isolated from parental L cells and gro29 cells were similar. The polypeptides denoted with asterisks were specific to infected cells and fractionated consistently with nucleocapsids and virions. By comparing these gels to those published previously (38), we determined that the upper and lower bands represent VP21 and VP22a. The material sedimenting in gro29 fraction 35 represents urea-insoluble material that was not efficiently removed in the step prior to centrifugation.

Although the nucleocapsid fractionation procedure gives an accurate assessment of the relative amounts of nucleocapsids present in the cells, we wanted to determine the number of intracellular particles that were also infectious. Cells were lysed in the absence of detergent, nuclei were removed, and extracts were fractionated on dextran T10 gradients. Total TCA-insoluble radioactivity in each fraction was determined, as was the number of infectious particles in selected fractions (Fig. 6A and B). In addition, samples were subjected to electrophoresis in polyacrylamide gels to detect the polypeptides sedimenting in the gradient (Fig. 6C). In L cells (Fig. 6B), fraction 12 contained 60% of the infectious particles and 85% of the infectious particles were in fractions 10 to 14. gD was detectable in these fractions (Fig. 6C), as were the two nucleocapsid proteins (asterisks). gro29 cell extracts fractionated differently, however. Whereas the peak of infectious particles was in the same fraction as in the L-cell gradient (fraction 12), the peak of radioactivity was at fraction 14 in the gro29 cell gradient (Fig. 6A). Analysis of the polypeptides in these fractions (Fig. 6C) revealed that a low number of polypeptides sedimented in the gradient, as expected for fractions enriched in virions. An analysis of the polypeptides in the L and gro29 cells revealed several differences. There were alterations in the polypeptides in the gB region of the gel, which were not analyzed further. The gro29 fractions were enriched in immature forms of gD (pgD), whereas L-cell fractions contained mostly mature gD. The identities of these polypeptides were confirmed by immunoprecipitation and Western blots (data not shown). Furthermore, most of the mass of radiolabeled gD was associated with the virion-enriched fractions, suggesting that a large portion of the intracellular gD was embedded in viral envelopes. It is clear from these results that newly formed particles were present in the cytoplasm of infected cells, and it appears that they were enveloped inasmuch as viral glycoproteins fractionated with the peak of infectivity. The apparent differences in the sedimentation observed between L and gro29 cells were not investigated further.

Although this procedure for isolating intracellular viral particles results in contamination of the sedimenting material with cellular polypeptides, it is useful for determining the infectivity of the intracellular particles. To determine the number of PFU in each fraction, samples of each gradient fraction were diluted in growth medium and used to inoculate monolayers of Vero cells. L-cell samples contained 270 PFU per cell, whereas gro29 cell samples contained 1.5 PFU per cell. These data and the data regarding total intracellular particles (Fig. 6) suggest that the lesion in gro29 cells inhibits or destroys the infectivity of the particles that are formed inside the cells, resulting in a decreased specific infectivity for the intracellular virions.

Immunofluorescence and electron microscopic analysis of infected cells. On the basis of these observations, we wanted to investigate the intracellular location of virions and glycoproteins. Cells were grown on cover slips, infected with HSV-1, and prepared for indirect immunofluorescence at 13 hpi. An anti-gD monoclonal antibody was used to detect gD on the cell surface and inside the cells after permeabilization with detergent (Fig. 7). Diffuse cytoplasmic staining was evident in infected L cells (Fig. 7A), with many discrete patches of gD scattered throughout the cytoplasm. These patches may represent virions in cytoplasmic vacuoles that were in transit to the cell surface prior to egress. In some cells, gD was concentrated in a juxtanuclear region which may contain the Golgi complex. These observations are consistent with biochemical data demonstrating that gD traversed the Golgi en route out of the cell (Fig. 3) and with the accumulation of gD-containing intracellular particles in the cytoplasm (Fig. 6).

The localization of gD in gro29 cells was very different from that of the parental L cells (Fig. 7B). In these cells, gD was concentrated in a juxtanuclear region and there was very little of the diffuse cytoplasmic staining visible in L cells. The majority of the cytoplasmic gD appeared to be in small round cytoplasmic vacuoles. There was also some reticular cytoplasmic staining evident, consistent with gD being present in the ER. We conclude that the intracellular distribution of gD was perturbed in these cells.

To determine whether there was a block to the appearance of viral glycoproteins on the surface of gro29 cells, cells were infected, fixed, and prepared for immunofluorescence without permeabilizing the cells. Comparisons of the cell surface staining (Fig. 7C and D) indicated that gD was transported to the cell surface in both L cells and gro29 cells. To determine the relative abundance of gD on the surface of gro29 cells compared with L cells, samples of infected cells were analyzed by flow cytometry in a fluorescence-activated cell analyzer (data not shown). To do this, monolayers of L cells and gro29 cells were infected with HSV-1 (MOI = 10) and harvested by rinsing in growth medium containing 10 mM EDTA. Mock-infected cells were also harvested for use as controls for nonspecific binding. Cells were rinsed and then stained with an anti-gD monoclonal antibody followed by a fluorescein-conjugated second antibody. The analysis of 10^4 L cells revealed a single population of cells with an average fluorescence 28-fold higher than the fluorescence in the uninfected-cell controls. By contrast, gro29 cells exhibited a bimodal distribution, with 80% of the cells eliciting an average fluorescence intensity equivalent to 9% of the infected L-cell population. The fluorescence of the remaining 20% of the gro29 cells was indistinguishable from the fluo-

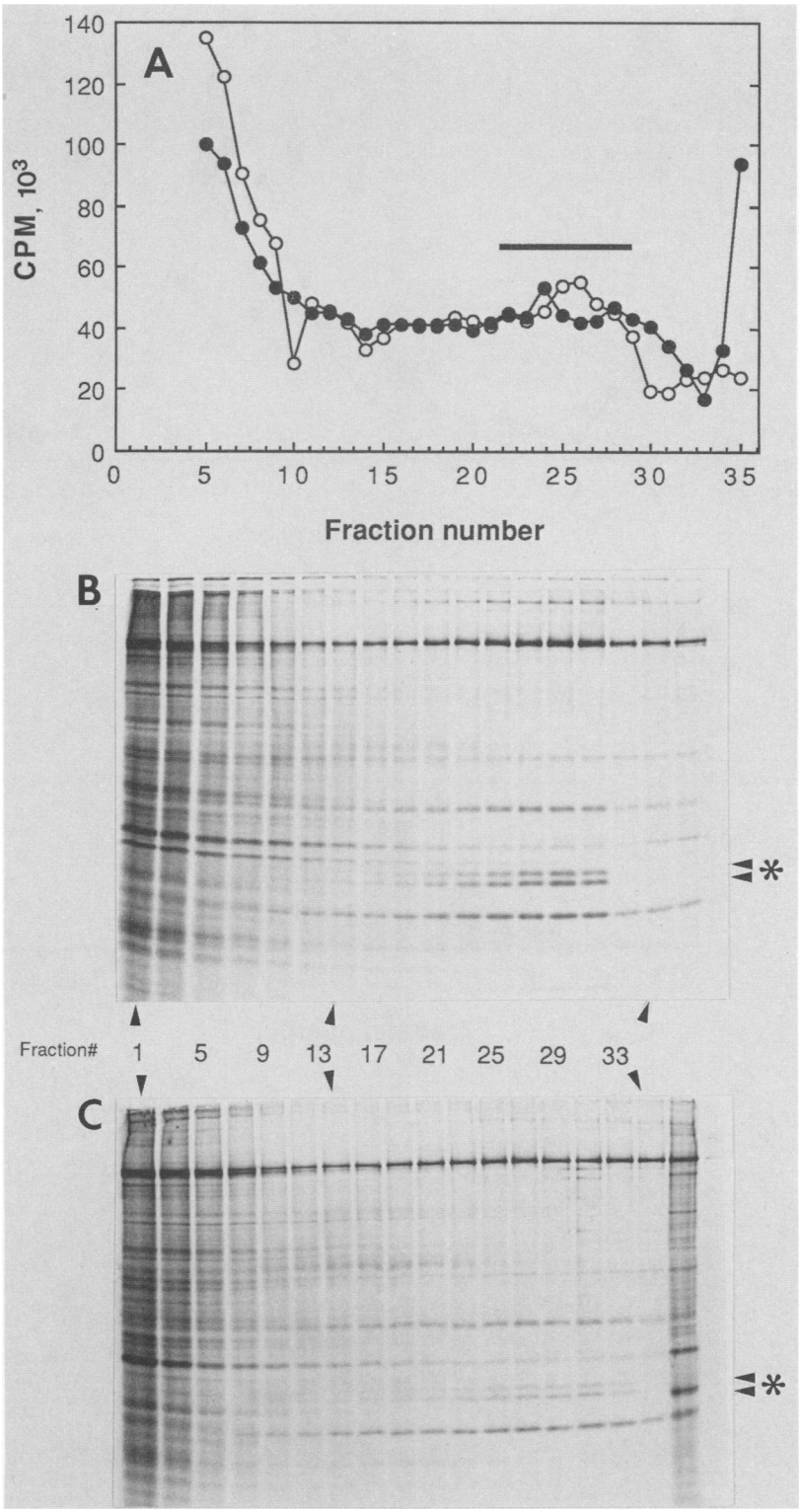

FIG. 5. Nucleocapsid assembly in L and gro29 cells. Parental L cells and gro29 cells infected with HSV-1 (MOI = 10) were labeled with [^{35}S]methionine (50 μCi/ml) from 2 to 18 hpi. Cell monolayers were harvested, and protein extracts were prepared with NP-40–deoxycholate extraction buffer. The extracts were sonicated, 0.5 M urea was added, and insoluble material was pelleted from the sample by low-speed centrifugation. The resulting extracts were layered onto a 10 to 40% sucrose gradient and centrifuged. The gradients were fractionated into 35 samples and analyzed. (A) Radioactivity in TCA-precipitable material for each fraction. The bar over fractions 22 to 29 represents the peak of nucleocapsids. Symbols: ○, L cells; ●, gro29 cells. (B and C) Autoradiograms of L cells (B) and gro29 cells (C) showing radiolabeled polypeptides present in odd-numbered fractions. Two nucleocapsid proteins that fractionate with nucleocapsids and whole virions are indicated (asterisk).

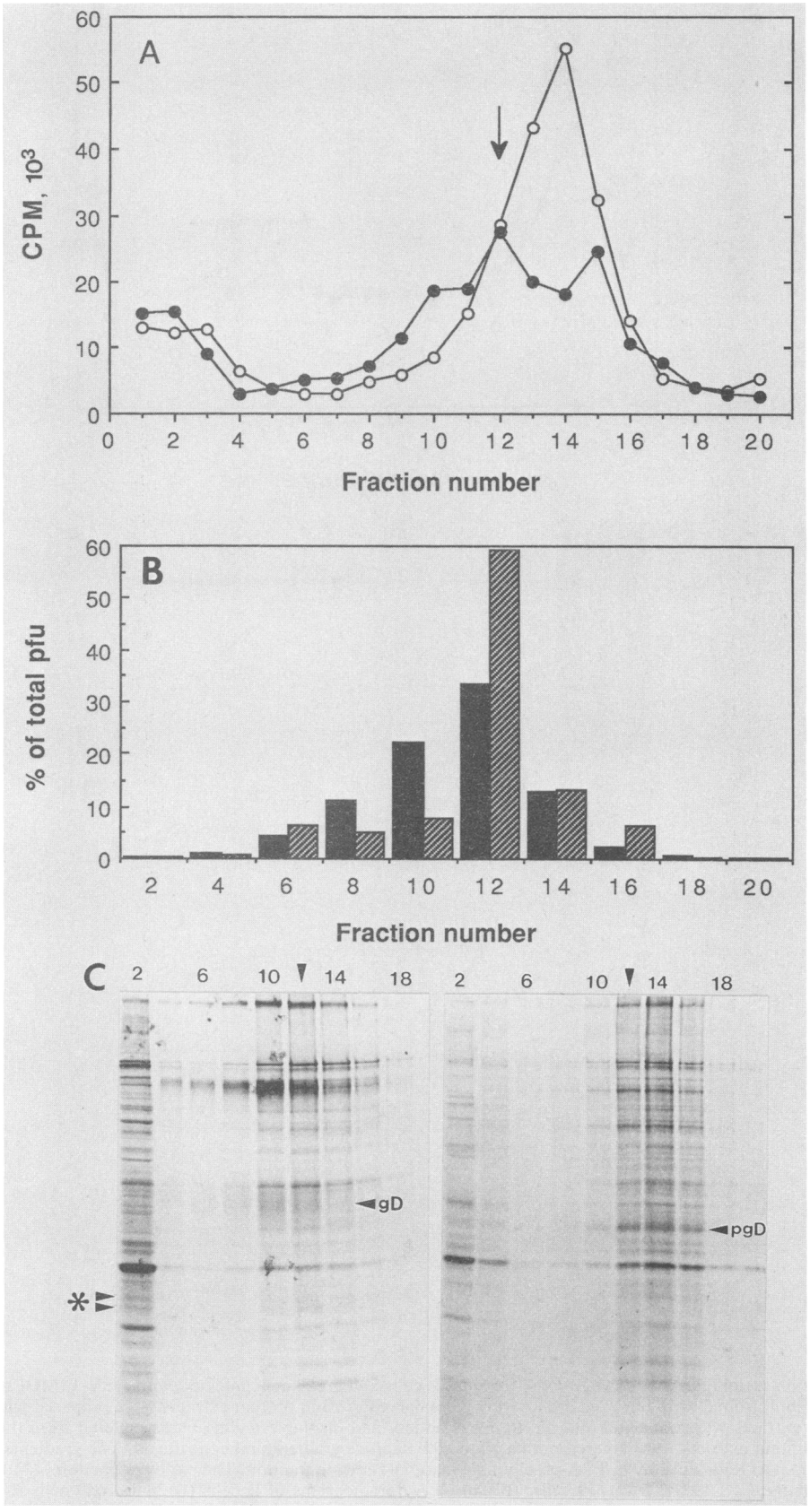
A
CPM, 10^3
Fraction number
B
% of total pfu
Fraction number
C
gD
pgD
*

rescence intensity of L cells. These results are consistent with the observation that gro29 cells were able to secrete proteins. We conclude that the flux of individual viral glycoproteins from the ER to the cell surface was perturbed only slightly in the mutant cell line when compared with the flux of viral particles out of the cells.

To determine the intracellular location of virions, infected L cells and gro29 cells were examined by electron microscopy. In infected L cells, large cytoplasmic vacuoles containing many virions were observed (Fig. 8A). An enlargement of a single vacuole is shown in Fig. 8C. These structures were not common in L cells and are shown to allow for comparison to the structures seen in gro29 cells. Infected gro29 cells contained numerous small vacuoles in the cytoplasm, many of which also contained enveloped viral particles (Fig. 8B and D). Whereas the large vacuoles in L cells were filled with particles, the vacuoles in gro29 cells were irregular in shape and contained few virions, and free nucleocapsids were often located adjacent to these vacuoles (Fig. 8D).

Figure 8E shows a confocal immunofluorescence micrograph of infected gro29 cells at 13 hpi stained with anti-gD antibody and a rhodamine-conjugated second antibody. In this procedure, decoration of the nuclear membrane and endoplasmic reticulum was well resolved, and gD was clustered in discrete locations of the cell. It is likely that this intense staining derived from the virion-containing vacuoles visible in the electron micrographs (Fig. 8F).

DISCUSSION

This report describes the maturation and transport of HSV-1 glycoproteins and virions in the mutant mouse cell line gro29. We have shown that the release of infectious virus from HSV-1-infected gro29 cells was diminished 2,000-fold due to a specific block in viral egress (Fig. 4). Although the assembly and envelopment of nucleocapsids occurred with high efficiency in gro29 cells, the low specific infectivity of the intracellular virus indicates that the maturation of the newly formed virions into infectious particles was impaired (Fig. 5 and 6).

We have shown that the viral particles which accumulate intracellularly in gro29 cells contain HSV-1 glycoproteins in their envelopes (Fig. 6). Analysis of the processing of HSV-1 gB and gD during infection indicates that these and probably all HSV-1-encoded glycoproteins were synthesized normally in gro29 cells and were modified by the addition of N-linked oligosaccharide moieties in the ER (Fig. 2A). The rate of oligosaccharide processing of the HSV-1 glycoproteins was lower in infected gro29 cells, however, since most of the newly-synthesized glycoproteins were slow to convert to endo H-resistant forms (Fig. 2B). Moreover, subcellular fractionation of gro29 cells revealed that newly made gD was underrepresented in the membranes of the Golgi complex at 13 hpi (Fig. 3). Despite this impediment, immunofluorescence experiments (Fig. 7D) and flow cytometry (data not shown) indicate that HSV-1 glycoproteins were transported to the cell surface during infection.

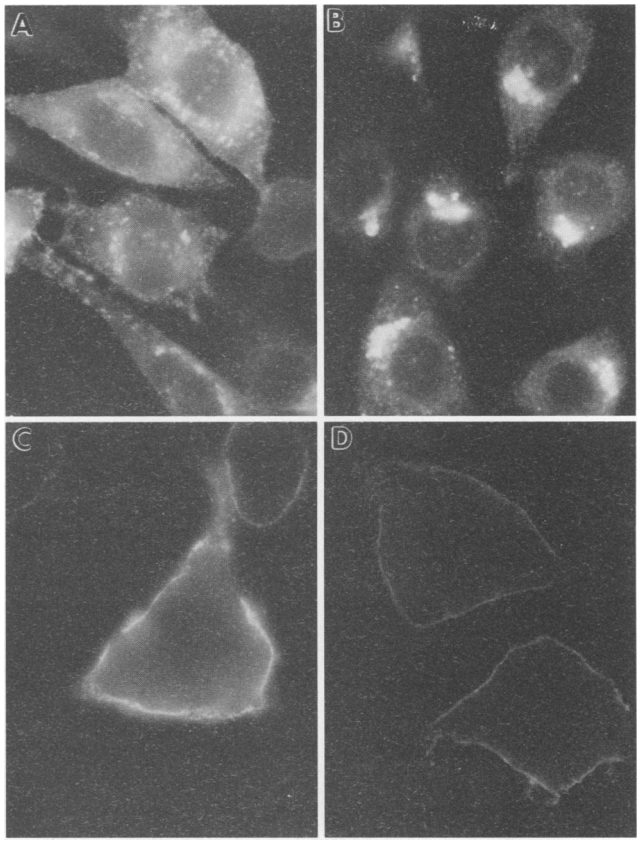

FIG. 7. Immunofluorescence analysis of HSV-1 gD in HSV-1-infected L and gro29 cells. Parental L and gro29 cells were grown on glass cover slips and infected with HSV-1 (MOI = 5). At 13 hpi, monolayers were fixed and prepared for immunofluorescence as described in Materials and Methods. The distribution of HSV-1 gD in permeabilized cells (A and B) or on the cell surface (C and D) of L cells (A and C) and gro29 cells (B and D) was detected by indirect immunofluorescence using an anti-gD monoclonal antibody, followed by a rhodamine-conjugated second antibody.

It has been shown previously that gro29 cells are defective in the transport and processing of glycoproteins (50). This property likely accounts for the slow processing of the HSV-1 glycoproteins that we observed in this study. What could account for the extreme block to virion egress in this cell line? Several models have been proposed for the maturation and egress of virions in HSV-infected cells. In one model, HSV-1 virions begin assembly in the nucleus, become enveloped as they exit the nucleus, and are carried to

FIG. 6. Detection of intracellular virions. Parental L cells and gro29 cells were infected with HSV-1 (MOI = 10) and incubated for 18 h in the presence of [^{35}S]methionine (50 μCi/ml). Cell monolayers were harvested, and whole-cell extracts were prepared by gentle homogenization in the absence of detergents. Cell debris and nuclei were pelleted from the extracts, which were then centrifuged for 1 h at 22,000 rpm through a 5 to 40% dextran T10 gradient. The gradients were fractionated, and samples were retained for further analysis. (A) Radioactivity in TCA-precipitable material. The arrow denotes the peak of infectious particles. Symbols: ●, L cells; ○, gro29 cells. (B) The number of PFU in each fraction was determined by limiting dilution analysis and plotted as the percent of total infectious particles in each fraction. Symbols: ▨, L cells; ■, gro29 cells. (C) A sample of every other fraction was subjected to SDS-polyacrylamide gel electrophoresis, and the radioactive polypeptides were detected by fluorography. The L-cell fractions are shown in the left lanes (fractions 2 to 18); the gro29 fractions are shown in the right lanes (fractions 2 to 18). The positions of gD and pgD, as determined by immunoprecipitation and Western blotting (not shown), are indicated.

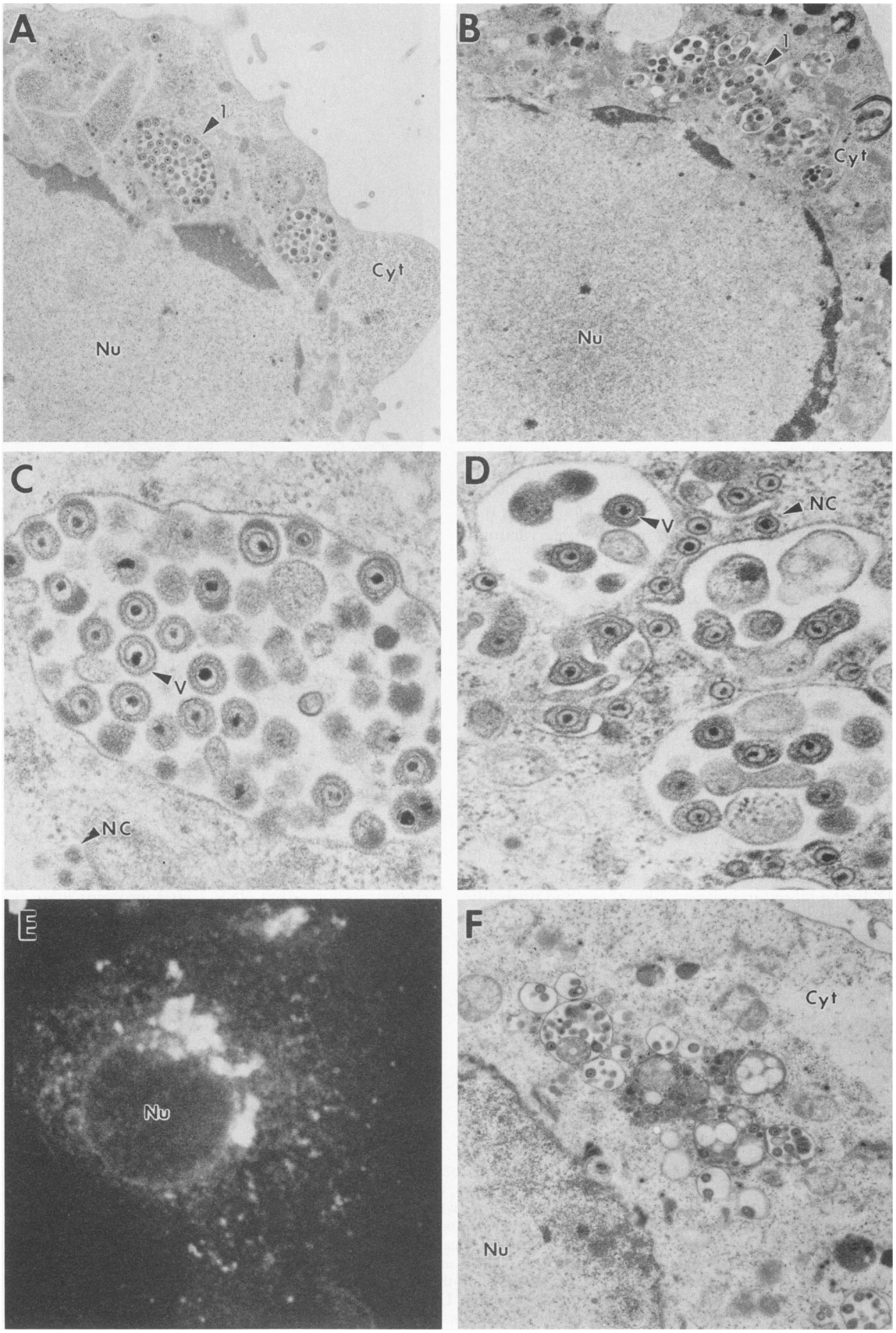
A
I
Cyt
Nu
B
I
Cyt
Nu
C
V
NC
D
V
NC
E
Nu
F
Cyt
Nu

the ER and Golgi apparatus and then to the plasma membrane in vesicles similar to those which carry newly made membrane glycoproteins and secreted proteins (21). Budding occurs at the nuclear membrane, where immature glycoproteins are more prevalent than the processed mature forms (12). Because virions released from infected cells contain mature glycoproteins, it is likely that the envelope glycoproteins are modified in the Golgi apparatus while resident in the virus membrane (21, 45). A second model proposes that cytoplasmic vacuoles and not the nuclear membrane are the predominant sites of envelopment within infected cells (35, 39). This second mechanism operates in the envelopment of another herpesvirus, varicella-zoster virus (23). Both models predict that perturbations in the secretory apparatus of infected cells could affect the maturation and transport of glycoproteins and virions. The fact that we observed a block to virus egress without a commensurate block in glycoprotein transport is unique to this cell line and suggests that virions and glycoproteins have different cellular requirements during the HSV-1 life cycle.

Somatic cell mutants defective in glycosylation enzymes can affect the transport and processing of HSV-1 glycoproteins, and in some instances the cells fail to produce normal amount of infectious virus. When mutant BHK cells defective in *N*-acetylglucosaminyltransferase I activity are infected with HSV-1, immature forms of several HSV-1 glycoproteins including gB and gD accumulate (10). The release of infectious HSV-1 particles from these cells is relatively normal, however, in contrast to our results for gro29. A different mutant cell line, which is defective in the glycosyltransferases that add terminal sugars to glycoproteins (51), displays altered HSV-1 glycoprotein forms upon infection with HSV-1 but is reduced only three- to fivefold in the release of viral particles (44). Although these cellular mutants are likely to have suffered multiple defects, the observation that cells defective in glycoprotein processing or transport are also affected in virus propagation suggests that a single lesion can impinge on both processes. The fact that we observed a novel phenotype with regard to virion egress in gro29 cells indicates that gro29 harbors a lesion distinct from those characterized previously.

Many of our observations suggest that the properties of gro29 cells are similar to those induced in HSV-1-infected cells treated with the ionophore monensin (21). Monensin has been shown to interfere with the processing of N-linked oligosaccharides (53), the addition of O-linked sugars to HSV-1 glycoproteins, the transport of HSV-1 glycoproteins from the Golgi apparatus to the plasma membrane, and the egress of virions (21). We have shown by a number of criteria that processing of N-linked oligosaccharides, the transport of glycoproteins, and the egress of virions are impeded in gro29 cells. The addition of O-linked sugars to the HSV-1 glycoproteins has not been investigated directly in this study, although the absence of the larger forms of the glycoproteins indicates that these modifications do not occur efficiently in gro29 cells (22). The subcellular fractionation of the secretory organelles of gro29 cells (Fig. 3) suggests that the failure to add O-linked sugars may arise from inefficient transport preventing the bulk of the newly made glycoproteins from entering the *trans* Golgi and the *trans* Golgi reticulum.

One of the most striking phenomena observed in HSV-1-infected gro29 cells and monensin-treated cells is the accumulation of virions in cytoplasmic vacuoles (Fig. 8). These vacuoles may represent intermediates in the pathway of virion egress. The electron micrographs (Fig. 8B and D) suggest that progeny virions produced in gro29 cells may be fusing with the membranes of the vacuoles in which they were contained. It is possible that the maldistribution of gD in the membranes of gro29 cells may allow the cells to be superinfected from within, resulting in excessive losses of progeny virions while they are in the process of being transported out of the cells. Alternatively, it may be that virions which are defective in some way are targeted to these vacuolar structures. Support for this notion comes from the observation that the virions contained in the vacuoles in gro29 cells were altered in their morphology when compared with L-cell virions (Fig. 8C and D). It is not known whether vacuoles of this type are Golgi derived, as suggested previously (21), and it is not clear why they are abundant in gro29 cells and monensin-treated cells.

We have also identified several important distinctions between the phenotypes of monensin-treated cells and gro29 cells. Treatment of HSV-1-infected cells with toxic concentrations of monensin does not block virion egress as effectively as we have observed for gro29 cells (21). Moreover, HSV-1 glycoproteins are not detectable on the cell surface of monensin-treated cells when analyzed by cell surface iodination (21), whereas we readily detected HSV-1 glycoproteins on the surface of infected gro29 cells by immunofluorescence (Fig. 7D) and flow cytometry. The capacity of gro29 cells to transport at least a portion of their glycoproteins to the cell surface likely accounts for their ability to grow in culture. These results suggest that the targets for monensin are distinct from those affected by the lesion in gro29 cells. It may be that the mutant properties common to monensin-treated and gro29 cells arise in all cells deficient in secretion.

What accounts for the difference in the trafficking of individual glycoproteins versus intact virions? Virus glycoproteins encoded by HSV-1 can exist as membrane-resident proteins anchored in cellular organelles or embedded in the virus envelope. Consequently, their cytoplasmic and transmembrane domains can reside in the virion or in the cytoplasm and organellar membranes of the infected cells. Although the molecular features that regulate the rate of virus transport through the cell have not been characterized, it is likely that the glycoproteins embedded in the viral envelope influence the trafficking of the viral particle. It may be the case that the interactions of the virion with the secretory organelles are impaired in the gro29 cells. The fact that the requirements for virion and glycoprotein transport are differentiated in gro29 cells suggest that they are differentiated in normal cells as well.

FIG. 8. High-resolution microscopy of HSV-1-infected L and gro29 cells. Parental L and gro29 cells were grown on Millicell HA inserts (Millipore) for 24 h prior to infection with HSV-1 (MOI = 5) or mock infection. Following inoculation, fresh DMEM containing 10% FBS was added and the infection was allowed to proceed for a further 18 h. For electron microscopy, cell monolayers were rinsed, fixed in glutaraldehyde, embedded, and sectioned. (A) HSV-1-infected L cells; (B) HSV-1-infected gro29 cells; (C and D) higher-magnification image of region 1 indicated in panels A and B, respectively; (E) confocal image of HSV-1-infected gro29 cells prepared as described in the legend to Fig. 5; (F) HSV-1-infected gro29 as in panel B prepared from a different sample showing HSV-1 particles in a cytoplasmic location. Nu, Nucleus; Cyt, cytoplasm; v, virus particle; NC, nucleocapsid.

It is worth noting that other L-cell mutants have been isolated previously which are unable to support the propagation of animal viruses. The mouse L-cell line CL3, a ricin-resistant derivative, is unable to support the growth of Sindbis virus (14, 15). Sindbis virus is an enveloped RNA virus comprising two glycoproteins. The cleavage of one of these, PE2 to E2, occurs prior to assembly and is required for virion formation. This cleavage is blocked in CL3 cells and may account for the failure of Sindbis virus to bud from the plasma membrane. Interestingly, when Sindbis virus-infected cells are treated with monensin, virus assembly takes place and enveloped particles can be found in monensin-induced cytoplasmic vacuoles (19). The observations that CL3 cells, gro29 cells and cells treated with monensin exhibit defects in the processing of glycoproteins and in the maturation and egress of diverse families of enveloped viruses argues strongly that common cellular components facilitate these events.

Regardless of the molecular basis of the gro29 phenotype, we are intrigued that this cell line is able to survive in culture. It suggests that the mutation in gro29 is leaky or occurs in a gene product whose function is not required for growth in culture medium. From these observations, we predict that it should be possible to interfere with protein trafficking so as to leave the host cell viable, while at the same time destroying the ability of herpes simplex virus to mount a productive infection.

ACKNOWLEDGMENTS

We thank H. Meadows and M. Weis for excellent technical assistance and M. Zweig and R. Philpotts for kindly providing monoclonal antibodies. We wish to acknowledge the Biotechnology Institute at the University of British Columbia for use of the confocal microscope. Special thanks to W. R. McMaster and G. B. Spiegelman for critical reading of the manuscript, and to "reviewer 2" who suggested the possibility that HSV-1 particles are fusing with internal membranes during infection of gro29 cells.

Support for this study was provided by grants from the Medical Research Council of Canada and the British Columbia Health Care Research Foundation to F.T.

LITERATURE CITED

1. **Ackermann, M., R. Longnecker, B. Roizman, and L. Pereira.** 1986. Identification, properties, and gene location of a novel glycoprotein specified by herpes simplex virus 1. Virology **50**:207–220.
2. **Balch, W. E., W. G. Dunphy, W. A. Braell, and J. E. Rothman.** 1984. Reconstitution of the transport of protein between successive compartments of the Golgi measured by the coupled incorporation of N-acetylglucosamine. Cell **39**:405–416.
3. **Balch, W. E., K. R. Wagner, and D. S. Keller.** 1987. Reconstitution of transport of vesicular stomatitis virus G protein from the endoplasmic reticulum to the Golgi complex using a cell-free system. J. Cell Biol. **104**:749–760.
4. **Beckers, C. J. M., D. S. Keller, and W. E. Balch.** 1987. Semi-intact cells permeable to macromolecules: use in reconstitution of protein transport from the endoplasmic reticulum to the Golgi complex. Cell **50**:523–524.
5. **Braell, W. A., W. E. Balch, D. C. Dobbertin, and J. E. Rothman.** 1984. The glycoprotein that is transported between successive compartments of the Golgi in a cell-free system resides in stacks of cisternae. Cell **39**:511–524.
6. **Buckmaster, E. A., U. Gompels, and A. C. Monson.** 1984. Characterization and physical mapping of an HSV-1 glycoprotein of approximately 115×10^3 molecular weight. Virology **139**:408–413.
7. **Burke, B., K. Matlin, E. Bause, G. Legler, N. Peyreiras, and H. Ploegh.** 1984. Inhibition of N-linked oligosaccharide trimming does not interfere with surface expression of certain integral membrane proteins. EMBO J. **3**:551–556.
8. **Bzik, D. J., B. A. Fox, N. A. DeLuca, and S. Person.** 1984. Nucleotide sequence specifying the glycoprotein gene, gB of herpes simplex virus type 1. Virology **133**:301–311.
9. **Campadelli-Fiume, G., M. T. Lombardo, L. Foa-Tomasi, E. Avitabile, and F. Serafini-Cessi.** 1988. Individual herpes simplex virus 1 glycoproteins display characteristic rates of maturation from precursor to mature form both in infected cells and in cells that constitutively express the glycoproteins. Virus Res. **10**:29–40.
10. **Campadelli-Fiume, G., L. Poletti, F. Dall'olio, and F. Serafini-Cessi.** 1982. Infectivity and glycoprotein processing of herpes simplex virus type 1 grown in a ricin-resistant cell line deficient in *N*-acetylglucosaminyl transferase I. J. Virol. **43**:1061–1071.
11. **Cohen, G. H., D. Long, J. T. Matthews, M. May, and R. Eisenberg.** 1983. Glycopeptides of the type-common glycoprotein gD of herpes simplex virus types 1 and 2. J. Virol. **46**:679–689.
12. **Compton, T., and R. J. Courtney.** 1984. Virus-specific glycoproteins associated with the nuclear fraction of herpes simplex virus type 1-infected cells. J. Virol. **49**:594–597.
13. **Darlington, R. W., and L. H. Moss.** 1968. Herpesvirus envelopment. J. Virol. **2**:48–55.
14. **Gottlieb, C., J. Baenziger, and S. Kornfield.** 1975. Deficient uridine diphosphate-N-acetylglucosamine:glycoprotein N-acetylglucosaminyltransferase activity in a clone of Chinese hamster ovary cells with altered surface glycoproteins. J. Biol. Chem. **250**:3303–3309.
15. **Gottlieb, C., S. Kornfield, and S. Schlesinger.** 1979. Restricted replication of two alphaviruses in ricin-resistant mouse L cells with altered glycosyltransferase activities. J. Virol. **29**:344–351.
16. **Hearing, J., M.-J. Gething, and J. Sambrook.** 1989. Addition of truncated oligosaccharides to influenza virus hemagglutinin results in its temperature conditional cell-surface expression. J. Cell Biol. **108**:355–365.
17. **Hearing, J., E. Hunter, L. Rodgers, M.-J. Gething, and J. Sambrook.** 1989. Isolation of Chinese hamster ovary cell lines temperature conditional for the cell-surface expression of integral membrane glycoproteins. J. Cell Biol. **108**:339–353.
18. **Hunt, L. A.** 1980. Altered synthesis and processing of oligosaccharides of vesicular stomatitis virus glycoprotein in different lectin-resistant Chinese hamster ovary cell lines. J. Virol. **35**: 362–370.
19. **Johnson, D. C., and M. J. Schlesinger.** 1980. Vesicular stomatitis virus and Sindbis virus glycoprotein transport to the cell surface is inhibited by ionophores. Virology **103**:407–424.
20. **Johnson, D. C., M. C. Frame, M. W. Ligas, A. M. Cross, and N. D. Stow.** 1988. Herpes simplex virus immunoglobulin G Fc receptor activity depends on a complex virus of two viral glycoproteins, gE and gI. J. Virol. **62**:1247–1254.
21. **Johnson, D. C., and P. G. Spear.** 1982. Monensin inhibits the processing of herpes simplex virus glycoproteins, their transport to the cell surface, and the egress of virions from infected cells. J. Virol. **43**:1102–1112.
22. **Johnson, D. C., and P. G. Spear.** 1983. O-linked oligosaccharides are acquired by herpes simplex virus glycoproteins in the Golgi apparatus. Cell **32**:987–999.
23. **Jones, F., and C. Grose.** 1988. Role of cytoplasmic vacuoles in varicella-zoster virus glycoprotein trafficking and virion envelopment. J. Virol. **62**:2701–2711.
24. **Kingsley, D. M., and M. Krieger.** 1984. Receptor-mediated endocytosis of low density lipoprotein: somatic cell mutants define multiple genes required for expression of surface-receptor activity. Proc. Natl. Acad. Sci. USA **81**:5454–5458.
25. **Kingsley, D. M., K. F. Kozarsky, L. Hobbie, and M. Krieger.** 1986. Reversible defects in O-linked glycosylation and LDL receptor expression in a UDP-Gal/UDP-GalNAc 4-epimerase deficient mutant. Cell **44**:749–759.
26. **Kingsley, D. M., K. F. Kozarsky, M. Segal, and M. Krieger.** 1986. Three types of low density lipoprotein receptor-deficient mutants have pleiotropic defects in the synthesis of N-linked, O-linked, and lipid-linked carbohydrate chains. J. Cell Biol. **102**:1576–1585.

27. **Kornfeld, R., and S. Kornfeld.** 1985. Assembly of asparagine-linked oligosaccharides. Annu. Rev. Biochem. **54**:631–664.
28. **Kuismanen, E., B. Bang, M. Hurme, and R. F. Pettersson.** 1984. Uukuniemi virus maturation: immunofluorescence microscopy with monoclonal glycoprotein-specific antibodies. J. Virol. **51**: 137–146.
29. **Kuismanen, E., K. Hedman, J. Saraste, and R. F. Pettersson.** 1982. Uukuniemi virus maturation: accumulation of virus particles and viral antigens in the Golgi complex. Mol. Cell. Biol. **11**:1444–1458.
30. **Kuismanen, E., J. Saraste, and R. F. Pettersson.** 1985. Effect of monensin on the assembly of Uukuniemi virus in the Golgi complex. J. Virol. **55**:813–822.
31. **Longnecker, R., S. Chatterjee, R. J. Whitley, and B. Roizman.** 1987. Identification of a herpes simplex virus 1 glycoprotein gene within a gene cluster dispensable for growth in cell culture. Proc. Natl. Acad. Sci. USA **84**:4303–4307.
32. **Matthews, J. T., G. H. Cohen, and R. J. Eisenberg.** 1983. Synthesis and processing of glycoprotein D of herpes simplex virus types 1 and 2 in an in vitro system. J. Virol. **48**:521–533.
33. **Morgan, C., H. M. Rose, M. Holden, and E. P. Jones.** 1959. Electron microscopic observations on the development of herpes simplex virus. J. Exp. Med. **110**:643–656.
34. **Nakano, A., M. Nishijima, M. Maeda, and Y. Akamatsu.** 1985. A temperature-sensitive Chinese hamster ovary cell mutant pleiotropically defective in protein export. Biochim. Biophys. Acta **845**:324–332.
35. **Nii, S., C. Morgan, and H. M. Rose.** 1969. Electron microscopy of herpes simplex virus. II. Sequence of development. J. Virol. **2**:517–536.
36. **Pfeffer, S. R., and J. E. Rothman.** 1987. Biosynthetic protein transport and sorting by the endoplasmic reticulum and Golgi. Annu. Rev. Biochem. **56**:829–852.
37. **Richman, D. D., A. Buckmaster, S. Bell, C. Hodgman, and A. C. Monson.** 1986. Identification of a new glycoprotein of herpes simplex virus type 1 and genetic mapping of the gene that codes for it. J. Virol. **57**:647–655.
38. **Rixon, F. J., M. D. Davison, and A. J. Davison.** 1990. Identification of the genes encoding two capsid proteins of herpes simplex virus type 1 by direct amino acid sequencing. J. Gen. Virol. **71**:1211–1214.
39. **Rodriguez, M., and M. Dubois-Dalcq.** 1978. Intramembrane changes occurring during maturation of herpes simplex virus type 1: freeze-fracture study. J. Virol. **26**:435–447.
40. **Saraste, J., G. E. Palade, and M. G. Farquhar.** 1986. Temperature sensitive steps in the transport of secretory proteins through the Golgi complex in exocrine pancreatic cells. Proc. Natl. Acad. Sci. USA **83**:6425–6429.
41. **Saraste, J., G. E. Palade, and M. G. Farquhar.** 1987. Antibodies to rat pancreas Golgi subfractions: identification of a 58-kD cis-Golgi protein. J. Cell Biol. **105**:2021–2029.
42. **Serafini-Cessi, F., and G. Campadelli-Fiume.** 1981. Studies on benzhydrazone, a specific inhibitor of herpesvirus glycoprotein synthesis: size distribution of glycopeptides and endo-β-N-acetylglucosaminidase H treatment. Arch. Virol. **70**:331–343.
43. **Serafini-Cessi, F., F. Dall'Olio, N. Malagolini, L. Pereira, and G. Campadelli-Fiume.** 1988. Comparative study on O-linked oligosaccharides of glycoprotein D of herpes simplex virus types 1 and 2. J. Gen. Virol. **69**:869–877.
44. **Serafini-Cessi, F. Dall'Olio, M. Scannavini, and G. Campadelli-Fiume.** 1983. Processing of herpes simplex virus-1 glycans in cells defective in glycosyl transferases of the Golgi system: relationship to cell fusion and virion egress. Virology **131**:59–70.
45. **Spear, P. G.** 1985. Glycoproteins specified by herpes simplex viruses, p. 315–356. *In* B. Roizman (ed.), The herpesviruses, vol. 3. Plenum Publishing Corp., New York.
46. **Stanley, P.** 1984. Glycosylation mutants of animal cells. Annu. Rev. Genet. **18**:525–552.
47. **Tooze, J., and S. A. Tooze.** 1985. Infection of AtT20 murine pituitary tumour cells by mouse hepatitis virus strain A59: virus budding is restricted to the Golgi region. Eur. J. Cell Biol. **37**:203–212.
48. **Tooze, J., S. Tooze, and G. Warren.** 1984. Replication of coronavirus MHV-A59 in sac cells: determination of the first site of budding of progeny virions. Eur. J. Cell Biol. **33**:281–293.
49. **Trowbridge, I. S., R. Hyman, and C. Mazauskas.** 1978. The synthesis and properties of T25 glycoprotein in Thy-1-negative mutant lymphoma cells. Cell **14**:21–32.
50. **Tufaro, F., M. D. Snider, and S. L. McKnight.** 1987. Identification and characterization of a mouse cell mutant defective in the intracellular transport of glycoproteins. J. Cell Biol. **105**:647–657.
51. **Vischer, P., and R. C. Hughes.** 1981. Glycosyl transferases of baby-hamster-kidney (BHK) cells and ricin-resistant mutants. N-glycan biosynthesis. Eur. J. Biochem. **117**:275–284.
52. **Weiss, M., and M. C. Horzinek.** 1986. Morphogenesis of Berne virus (proposed family Toroviridae). J. Gen. Virol. **67**:1305–1314.
53. **Wenske, E. A., M. W. Bratton, and R. J. Courtney.** 1982. Endo-β-*N*-acetylglucosaminidase H sensitivity of precursors to herpes simplex virus type 1 glycoproteins gB and gC. J. Virol. **44**:241–248.